Journal of Geosciences, Osaka City University
Vol. 39, Art. 5, p.83–110
March, 1996

Sedimentary Evolution of the Ordovician Basin in Central Ningxia, North China

LIU Jianbo*, AN Taixiang** and ZHENG Zhaochang***

(with 7 Figures and 2 Tables)

Abstract

During Ordovician times the central Ningxia area was situated in the middle-western passive margin of the Sino-Korean Platform. Deposition here was controlled by both eustasy and tectonic activity.

Until the late Arenigian of Early Ordovician, carbonate platforms were well developed in this area. At least four long-term transgressive-regressive cycles, which are interpreted as third-order sequences, have been recognized on the basis of the stacking patterns of carbonate platform lithofacies associations. Sequence boundaries there were generated by either exposure or by the drowning of the carbonate platforms in central Ningxia.

From the end of the Arenigian, this area underwent transition from stable carbonate platforms to an active foreland basin in response to the increasing activity of the North-Qilian Fold Belt. In the western study area, the transitions are marked by the basin-marginal lithofacies associations, firstly deposited in Miboshan, then extending to Qingshan and Yantongshan in turn. Meanwhile, deposition in Qinglongshan was still dominated by carbonates but became deepening upwards in the long term (although interrupted by shallowing events). From the Middle Ordovician, terrigenous supplies increased, and basinal graptolitic shale and basin-marginal clastics prevailed in the middle and eastern parts of central Ningxia before being uplifted.

Key Words: Ordovician, sequences, paleogeography, central Ningxia.

Introduction

The Ordovician succession is well exposed in central Ningxia (Fig. 1), and is represented by a wide variety of lithofacies and lithofacies associations, from peritidal carbonates to basinal shales. It thus provides a good opportunity to study the development of sequences in the Ordovician.

In the Ordovician, central Ningxia was situated on the middle western Sino-Korean passive margin in central Ningxia (Fig. 1). Further understanding of the tectonic history between the Sino-Korean Platform and the North-Qilian Fold Belt depends largely on a more detailed sedimentological study of the Ordovician succession and the paleogeography of central Ningxia. Until now, however, sedimentary evolution of the Ordovician in central Ningxia, especially in the western study area, has been poorly documented.

On the basis of an extensive outcrop analysis, consisting of the measurement of

* Department of Geosciences, Osaka City University, Sugimoto 3–3–138, Sumiyoshi-ku, Osaka 558, JAPAN
** Department of Geology, Peking University, Beijing 100871, P.R. CHINA
*** Bureau of Geology and Minerals Resource of Ningxia, Yinchuan, Ningxia 750021, P.R. CHINA

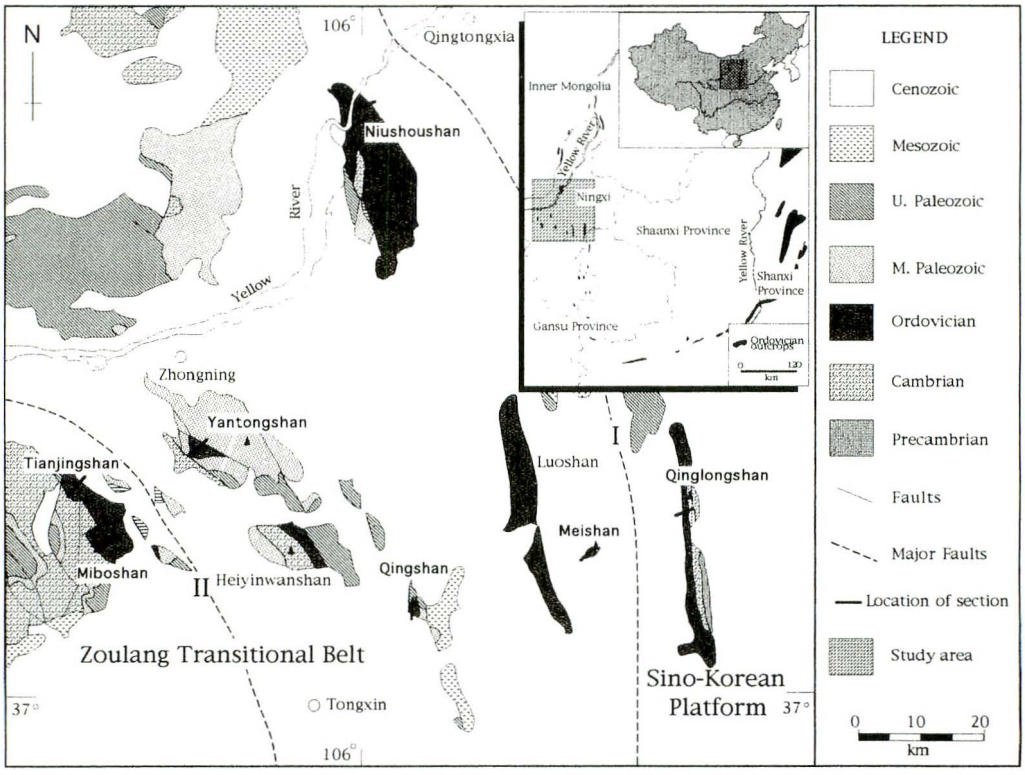

Fig. 1. Generalized geological map of central Ningxia showing Ordovician outcrops, modified from HUO *et al.* (1989). The major northwestward-trending deep faults are named as: I-Longshoushan-Liupanshan major fault, and II-Sapotou-Tongxin major fault. The former separates central Ningxia into two tectonic provenances. The inset maps show the location of the Ordos Basin in China and the location of the study area in Ordos Basin, respectively.

seven sections, this work proposes (i) to present a revised stratigraphic description of the Ordovician sequences in this area; (ii) to provide detailed relative sea-level curves deduced from the stacking patterns of the lithofacies and lithofacies associations; and (iii) to illustrate the episodes of sedimentary evolution, which consist of successive, genetically related units.

Structural and Stratigraphic Settings

The Ordovician of the study area is preserved in two major tectonic provenances (Fig. 1). The Qinglongshan section and surrounding areas in the east was the marginal part of the Sino-Korean craton; the western part, with deformed strata, lies within the Zoulang Transitional Belt of the North-Qilian Fold Belt, where the autochthonous shallow-water carbonates were overlain by the allochthonous deep-water deposits after the Llanvirnian or later. These two major tectonic provenances are separated by the Longshoushan-Liupanshan major deep fault, which has been recognized by geophysical

data (HUO *et al.*, 1989).

The Middle to Late Cambrian rifting of central Ningxia is indicated by thick, syn-rift deposits in the Zoulang Transitional Belt of the North-Qilian Fold Belt (Xiangshan Group, see in CUI *et al.*, 1985). The transition from rift to passive margin may have occurred at the end of the Late Cambrian as shown by the overlying Lower Ordovician shallow-water carbonates (Xialingnangou Formation and overlying strata, see in AN and ZHENG, 1989; LIU, 1991). The period following was characterized by the thermal subsidence. From the Llanvirnian of the Early Ordovician, the passive margin became more active due to the early collision of the North-Qilian Fold Belt with Sino-Korean Platform. This area may have been totally elevated above sea-level after the early Caradocian of the Middle Ordovician.

Age determinations and correlations for shallow-water carbonate strata of the Early Ordovician in central Ningxia were made predominantly on the basis of conodont biozones or assemblage-zones (AN and ZHENG, 1989; AN and ZHENG, unpub. data; LIU, 1991). Based on the conodont data, LIU (1991) redefined the Tianjingshan Formation (formally definited as Arenigian shallow-water carbonates) as consisting of three successions separated by faults. He named them the Xialingnangou Formation (early Tremadocian shallow-water carbonates), the Tianjingshan Formation (Arenigian shallow-water carbonates), and the Wangjiayuanzi Formation (Llanvirnian shallow-water carbonates) (See LIU, 1991 for additional detailed descriptions of conodont fauna and biostratigraphic correlation). Table 1 provides a biostratigraphic correlation scheme on local and global scales.

The significant work on Ordovician graptolites of this area (GE *et al.*, 1991) has provided another biostratigraphic control, and it is especially useful in siliciclastic strata developed from the Llanvirnian. The synthetic stratigraphic framework of central Ningxia is presented in Fig. 2.

Lithofacies and Lithofacies Associations

A broad spectrum of lithologies is present in the Ordovician of central Ningxia, which may have been deposited in peritidal to basinal settings. We describe below the lithofacies in terms of bedding characteristics, textures and sedimentary structures (Table 2), and group them into lithofacies associations, based on inferred genetic relationships.

Peritidal Lithofacies Association

Rocks of the peritidal lithofacies association are predominantly cryptalgal laminites, collapse breccia, dolomitic siltstone (e.g., Fig. 4-A), argillaceous fine-crystal dolostone and thin-bedded dolomitized intervals with no remnant primary depositional features.

Table 1. Conodont assemblages established from the Ordovician of central Ningxia, and its correlational scheme, with chronological and biostratigraphic divisions on local and global scales. Absolute age, in million years, after Harland *et al.* (1989). The graptolite biozones in Britain after Williams *et al.* (1972) and Fortey *et al.* (1995); conodont biozones from Baltoscandia after Lindström (1971) and Bergström (1977); conodont assemblage-zones in North China after An and Zheng (1989); and conodont assemblage-zones from central Ningxia after Liu (1991).

Time Scale	Era & Epoch		Graptolite biozone	Conodont biozone		
			Britain	Baltoscandia	North China	W. Ordos Basin
(Ma) 460	Upper Ord.	Carodoc	*Climacograptus peltifer*	*Amorphognathus tvaerensis*	*Tasmanognathus sishuiensis-Erismodus typus*	Hiatus
			Nemagraptus gracilis	*Pygodus anserinus*		Not yet established
	Middle Ordovician	Llandeilo	*Glypotograptus teretiusculus*		*Scandodus handanensis*	
470		Llanvirn	*Didymograptus murchisoni*	*Pygodus serrus*	*Aurilobudus serratus*	*Eoplacognathus reclinatus*
				Eoplacognathus suecicus	*Plectodina onychodonta*	*Eoplacognathus foliaceus*
			Didymograptus bifidus	*Amorphognathus variabilis*	*Eoplacognathus suecicus-Acontiodus? linxiensis*	*Pygodus anitae*
	Lower Ordovician	Arenig	*Didymograptus hirundo*	*Microzarcodina flabellum*	*Plectodina fragilis*	*Periodon aculeatus*
480			*Isograptus gibberulus*	*Paroistodus originalis*	*Tangshanodus tangshanensis*	*Rhipidognathus laiwuensis*
				Prionodus navis		
				Prionodus triangularis		
			Didymograptus nitidus	*Oepikodus evae*	*Aurilobodus leptosomatus-Loxodus dissectus*	*Aurilobodus leptosomatus-Loxodus dissectus*
			Didymograptus deflexus		*Jumudontus gananda-S colopodus sunanensis*	
490			*Tetragraptus approximatus*	*Prioniodus elegans*	*Paraserratognathus paltodiformis*	Hiatus
				Paroistodus proteus	*Serratognathus extensus*	
					Serratognathus bilobatus	
		Tremadoc	?	*Drepanoistodus deltifer*	*Scalpellodus tersus*	
500			*Bryograptus*	?	*Glyptoconus quadraplicatus-Scolopodus opimus*	
			Dictyonema flabelliforme	*Cordylodus intermedius*	*Cordylodus rotundatus-Rossodus manitouensis*	
					Utahconus beimataoensis-Monocostodus sevierens	Not yet established
510	Cambrian					

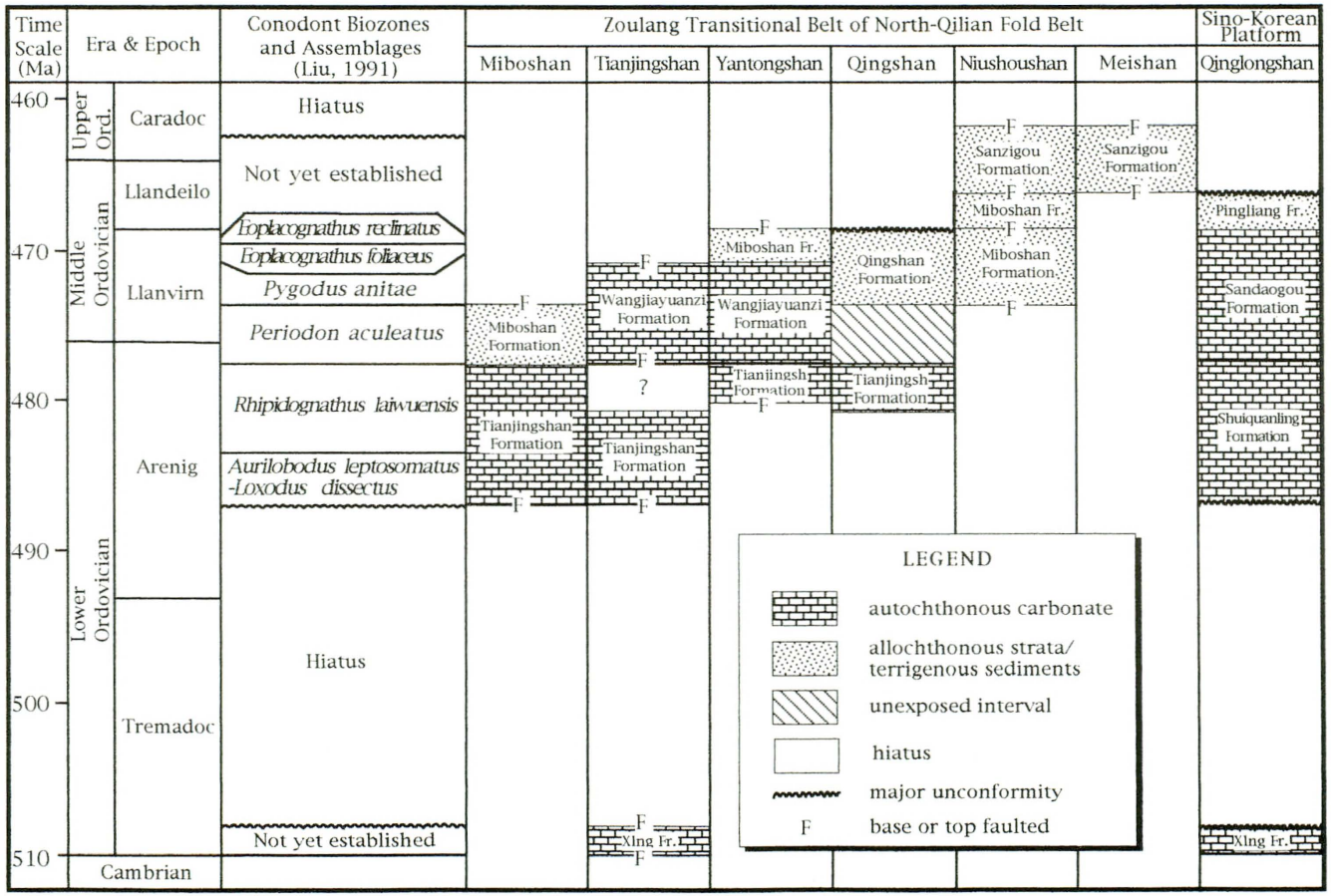

Fig. 2. Chronostratigraphic chart of the Ordovician in central Ningxia. Geographical location of the sections shown in Fig. 1. * Xln Fr. is abbreviated from Xialingnangou Formation.

Table 2. Descriptions of characteristic lithofacies within lithofacies associations.

Peritidal Lithofacies Association

Cryptalgal Laminite (Fig. 3-A): tan to dark grey, 0.5–3 m thick; micrite, with rare small peloids; fine, planar to wavy to discontinuous lamination; rare mudcracks; irregular and laminar fenestrae; commonly completely dolomitized.

Collapse Breccia (Fig. 3-B): tan to grey, 0.2–2 m thick; laterally discontinuous beds of angular intraclasts in a calcrete matrix; intraclasts often poorly sorted and rounded, no preferred orientation or grading.

Dolomitic Siltstone (Fig. 4-A): tan to yellow-orange, brown-weathering, less than 0.3 m thick; quartzose silt; planar to wavy lamination, occasionally interbedded with dolomitic mudstone.

Argillaceous Fine Crystal Dolostone: light tan, thin- to medium-bedded, occasionally laminated; commonly overlying the subtidal or intertidal sediments, the cap of peritidal cycles.

Shallow Subtidal Lithofacies Association

Peloidal Grainstone (Fig. 5-A): light grey to grey, thick-bedded, up to 10 m in thickness; peloids commonly well-rounded and micritic, cemented by granular sparry cement; occasionally with small intraclasts and robust broken trilobites, echinoderms; cross-laminated; transitional with cyclic peritidal carbonates.

Peloidal Packstone: light grey to grey, thick-bedded, in thickness up to 12 m; peloids usually well-rounded and micritic; occasionally with small intraclasts and robust fossils; commonly bioturbated.

Deeper Subtidal Association

Bioturbated Lime Mud-Wackestone (Fig. 3-D, 5-B): grey to dark grey, medium- to thick-bedded, up to 14 m in bed thickness; grains consisting of peloids and fossils, e.g., trilobites, echinoderms, gastropods, ostracods; extensively bioturbated; commonly cherty.

Peloidal Wackestone-Packstone: grey to dark grey, thin- to medium-bedded, less than 0.5 m thick; commonly with sharp erosional base; Grains include peloids and skeletons of trilobites, echinoderms, gastropods; intraclasts commonly near base of units.

Lime Mudstone (Fig. 5-C): grey to dark grey, thin- to medium-bedded; micrite, commonly with terrigenous clays; less than 10 percent gains and open-sea fossils, e.g., trilobites, echinoderms, gastropod, ostracod; occasionally bioturbated.

Nodular Argillaceous Mud-Wackestone (Fig. 3-C): medium to dark grey, 0.5 to 6 m in thickness; discontinuous, nodular, wavy and thin-bedded, recessive weathering; variable intermixed textures from lime mudstone to skeletal peloidal wackestone, micrite with thin shell fossils e.g., trilobites, occasionally bioturbated.

Basin-Marginal Lithofacies Association

Carbonate Megabreccia/Conglomerate (Fig. 4-C, D): beds up to tens of meters in thickness; typically clast-supported, poorly sorted and lack grading, but commonly oriented; the megabreccia or conglomerates are angular to rounded, compositionally containing a mixture of peloidal grainstone/packstone, thin-bedded lime mudstone, siltstone clasts, etc.; lower contacts planar to gently undulatory; beds laterally persistent.

Terrigenous Clastic Turbidite (Fig. 4-B, 5-D): composed of feldspar sandstone, siltstone and/or mudstone. Sandstone: olive green to dark grey (brown-weathering), up to 2 m in thickness, graded bedding/parallel bedding commonly Bouma division Ta, Tb. Siltstone: olive green to grey, convolute bedding/cross-bedding, Bouma division Tc, Td. Shales: color varied, planar laminated, common Bouma division Td or Te.

Lime Mudstone (Fig. 5 E): medium grey to dark grey, thin-bedded, insoluble residues (quartz silt and clay) commonly less than 15 percent; burrows rare to absent, with grading generated by low-concentration turbidites; occasionally yielding fine-grained intraclasts and soft-deformed conglomerates.

Basinal Lithofacies Association

Lime Mudstone (Fig. 5 F): medium grey to dark grey; primary parallel lamination well preserved; rare burrows and no evidence for wave activity; bioclastic components dominated by radiolaria with rare fine trilobites; occasionally cherty.

Graptolitic Shale: dark grey to olive green, with continuous planar laminations; occasionally fine trilobites, phosphatic brachiopod fragments, and graptolites; burrows absent; commonly interbedded with siltstone.

Beds are about 0.2–1.5 m thick. Mudcracks occasionally occur. Peritidal lithofacies associations are recognized from the lower Shuiquanling Formation of Qinglongshan, and from the Tianjingshan Formation of the Zoulang Transitional Belt. This association is commonly dolomitized and interbedded with thick-bedded peloidal grainstone/packstone and/or bioturbated lime mudstone/wackestone.

The irregular and laminar fenestae in cryptalgal laminites are generally referred to as being the remains of algal mats (JAMES, 1984). Together with occasionally observed mudcracks, cryptalgal laminites may be deposited in intertidal settings (PRATT and JAMES, 1982). The textures of collapse breccias (Table 2) suggest that the formation of breccias may be caused by collapse after dissolution of overlying strata, especially evaporates. Such textures can be used to indicate deposition in upper intertidal to supertidal environments. Thus, the sediments grouped here into the peritidal lithofacies association indicate deposition on an arid tidal flat in environments similar to those in the modern Persian Gulf and Shark Bay (HARDIES and SHINN, 1986).

Shallow Subtidal Lithofacies Association

The shallow subtidal lithofacies association is typically composed of thick-bedded, peloidal grainstone and peloidal packstone as well as minor skeletal wackestone to grainstone interbeds. Lime mudstone is rare to absent, and when present is deposited mainly at the base of meter-scale, upward-shallowing cycles. Rocks of this association are in beds 0.3–3.5 m thick. They commonly bear more than 65 percent peloids and/or intraclasts, more or less bioclastics and are cemented by granular sparry calcite. Cross-bedding is relatively rare, but beds are commonly bioturbated. Similarly to the peritidal lithofacies associations, the shallow subtidal lithofacies association is concentrated in the Xialingnangou and Tianjingshan Formations of the Zoulong Transitional Belt, and in the Shuiquanling Formation of Qinglongshan. However, compositions of this association vary merely from section to section. In Qinglongshan, for example, peloidal packstone is well developed instead of peloidal grainstone, and in the Zoulong Transitional belt, grainstone dominates this lithofacies association.

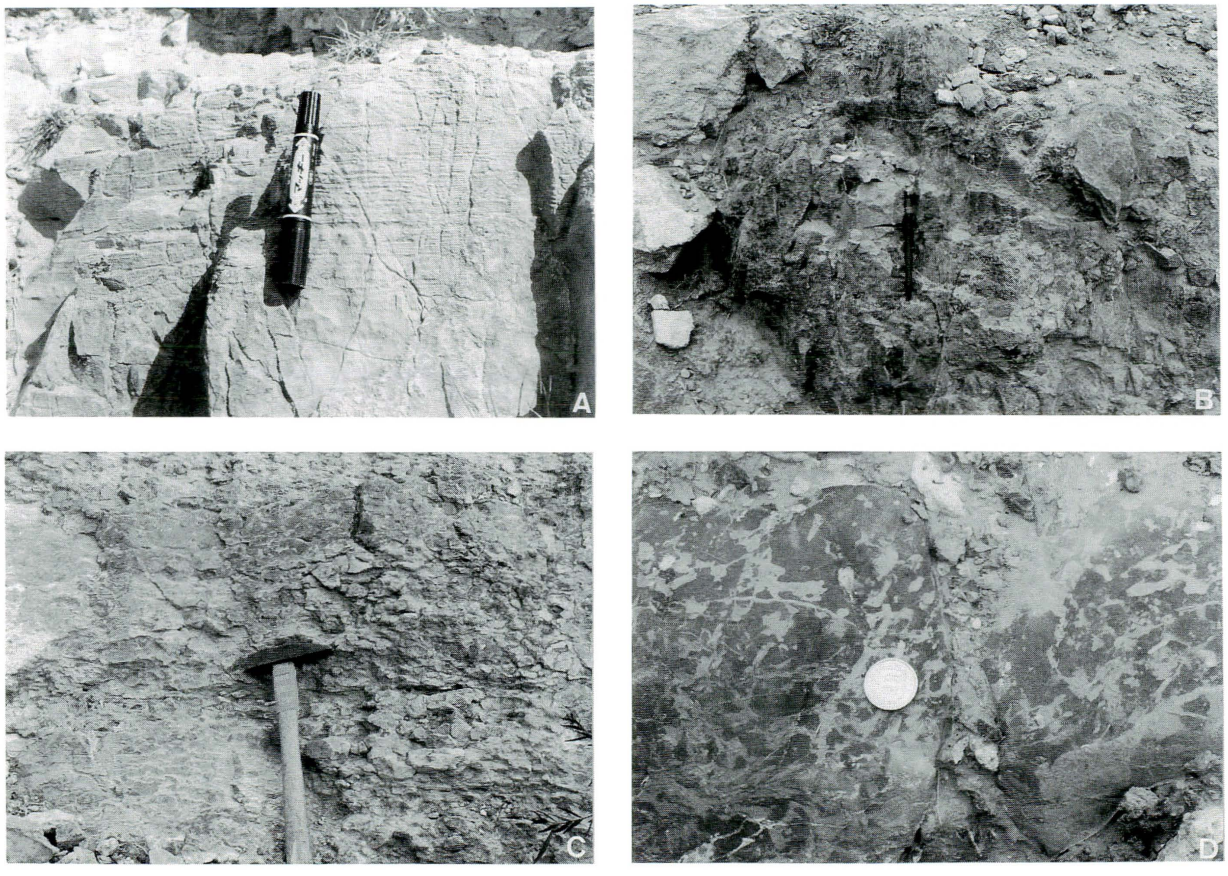

Fig. 3. Field photographs for various lithofacies. A-Planar-wavy, dolomitic cryptalgal laminite overlying the thick-bedded dolomitic peloidal packstone. B-Solution-collapse breccia with coarse quartz sands. C-Argillaceous nodular lime mudstone. D-Massive to thick-bedded bioturbated mud-wackestone. Individual burrows are mud-filled, and dolomitized.

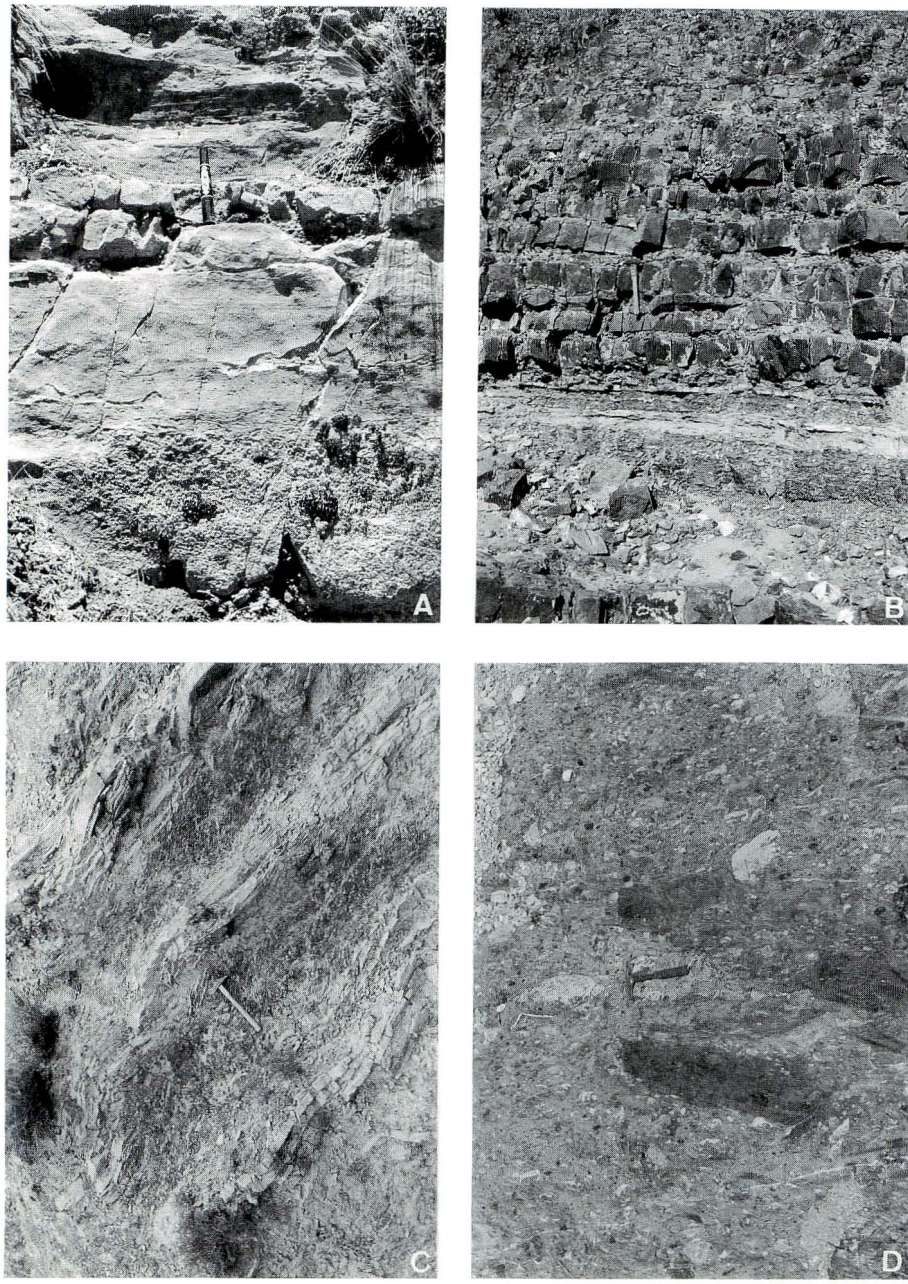

Fig. 4. Field photographs of various lithofacies. A-Dolomitized siltstone overlying peloidal grain-packstone. B-Intercalated medium- to fine-grained sandstone/siltstone and shale with Bouma divisions. C-Black shales and siltstone with calcium turbidite interbeds. D-Polymict conglomerate with limestone, dolostone and siltstone clastics.

Thick grainstone/packstone is interpreted as shoal deposits, though only some cross-bedding was observed. Rounded and well-sorted peloids and sparry cements indicate depositions by wave reworking in water depths from sea-level to fair-weather wave-base (de RAAF *et al.*, 1977; BOVA and READ, 1987). Plausible Holocene analogs for the depositional setting of this lithofacies association are the vast, interior, shallow subtidal shelves of the Florida and Bahamian platforms (ENOS and PERKINS, 1977; HINE *et al.*, 1981). Such grainstones correspond to the "keep-up" phase in the sense of KENDALL and SCHLAGER (1981), and may be well developed in highstand systems tracts (BURCHETTE *et al.*, 1990; TUCKER *et al.*, 1993) of a sequence.

Deeper Subtidal Lithofacies Association

The deeper subtidal lithofacies association typically consists of bioturbated mud-wackestone, thin-bedded lime mudstone, and nodular argillaceous mud-wackestone. It is commonly shaly or argillite enriched. The strata of this association are in beds 0.1–14 m thick, commonly bioturbated, and contain more or less bioclastics, e.g., trilobite, echinoderm, gastropod, cephalopod. Fine-grained peloidal pack-wackestones occasionally occur in this lithofacies association, but are distinguished from those of the shallow subtidal association by thinner beds and containing more matrix. Tidal-flat caps or subaerial exposures are rarely intercalated with rocks in this association.

Bioturbated mudstone-wackestone (Fig. 3-D) and fine-grained peloidal wackestone represent depositional environments similar to those documented in the modern Bahamas by PURDY (1963). The nodular, argillaceous mud-wackestone (Fig. 3-C) may be deposited on the middle ramp, between bioturbated lime mud-wackestone and deeper water siliciclastic muds (AIGNER, 1985). Nodules may have been formed early by submarine lithofication under weak bottom currents (MULLINS *et al.*, 1980) or may be the result of late pressure solution and physical compaction (WANLASS, 1979).

The presence of abundant burrows and open-sea fossils (Fig. 5-C) suggests that the sediments of this association were deposited in open-marine subtidal settings, and lime mud-rich texture in the rocks suggests they were formed within low-energy settings, especially below the zone of storm wave reworking.

Basin-Marginal Lithofacies Association

The basin-marginal lithofacies association consists of various lithofacies, e.g., terrigenous turbidites, carbonate megabreccia/conglomerates, carbonate slumps, and thin-bedded lime mudstone.

The basin-marginal clastics are characterized by grey-green (brown-weathering) to dark grey, interbedded greywackes, feldspathic sandstone (Fig. 5-D), siltstone, and shale. These deposits commonly contain partial to complete Bouma divisions (Ta-Te). The contacts between individual Bouma sequences are sharp and planar, and individual beds are laterally persistent as far as the exposed outcrop. Sandstone contains mainly Ta and Tb, and siltstone commonly yields Tc and Te (Fig. 4-B). Flute casts

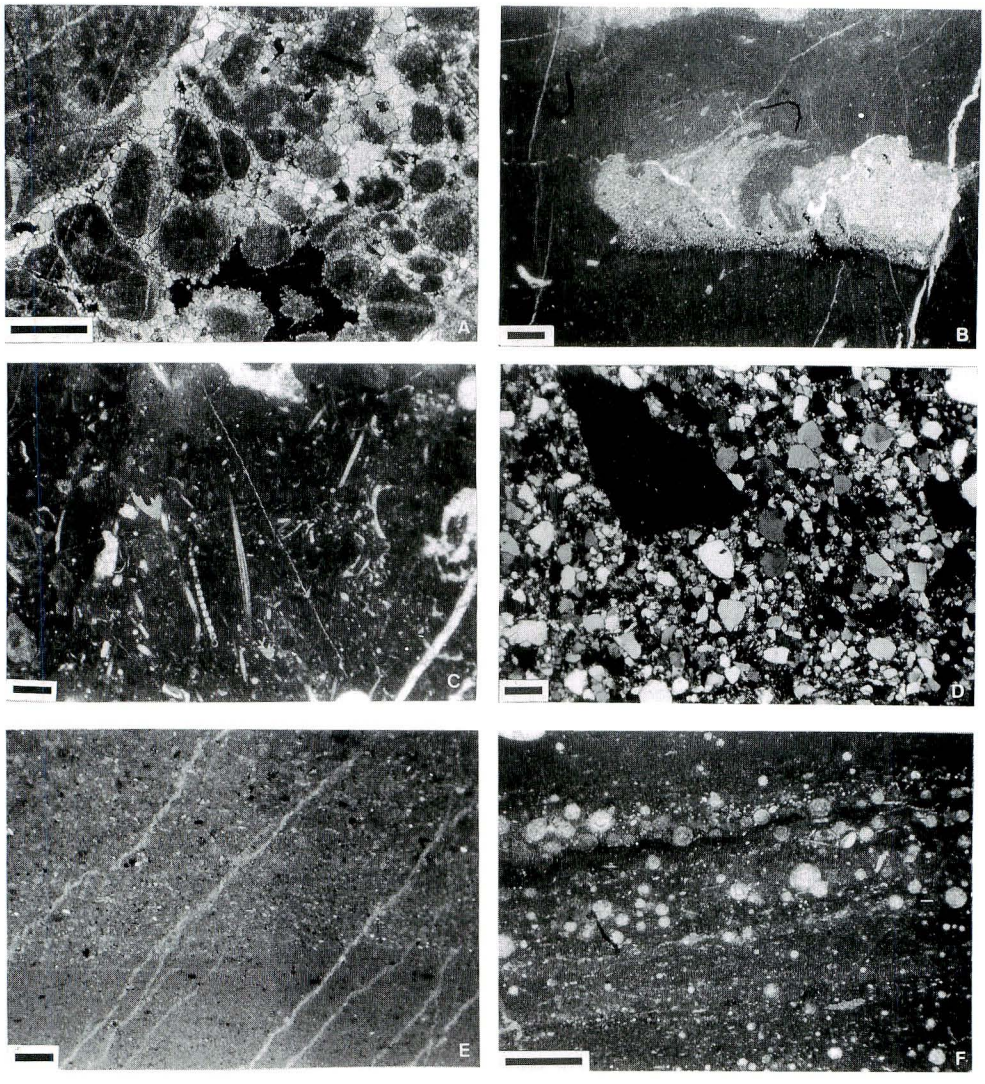

Fig. 5. Microscope photographs of various lithofacies. A-Peloidal grainstone with calcitic sparry cements. B-Burrow with back-packing structure in lime mudstone. C-Skeletal wackestone containing diversified bioclastics, e.g., echinoderms, trilobites, sponge spines. D-Coarse quartz sandstone with siltstone, peloidal grainstone conglomerates. E-Lime mudstone and overlying fine-grained turbidite. F-Lime mudstone with calcitized radiolarians. Solid bars in photographs represent the length of 0.5 mm.

are also abundant at the bottom of a Bouma sequence. The basin-marginal siliciclastics were predominately developed in the lower and middle Miboshan Formation and the Sanzigou Formation of Niushoushan during the Llanvirnian, and in the Niushoushan-Luoshan Trough after the Middle Ordovician.

The carbonate megabreccia/conglomerates in this lithofacies association have various textures (Table 2), and can be grouped into two types, based on clast lithologies. Polymict

breccias/conglomerates consist mainly of clasts (Fig. 4-D) transported from different depositional settings or even from different stratigraphic horizons. For example, the carbonate conglomerates in the Miboshan Formation of Yantongshan are composed of peloidal grainstone-packstone, bioturbated lime mudstone and thin-bedded lime mudstone, and minor siliciclastics, and they contain "chaotic" conodont fauna ranging from Late Cambrian to Llanvirnian of the Early Ordovician. In contrast, oligomict breccia/conglomerates consist predominantly of rounded to tabular lime mudstone clasts in a lime mud matrix.

Many features of carbonate megabreccia/conglomerates are recognized in Holocene and ancient submarine mass flows formed by major collapses and debris flows (CREVELLO and SCHLAGER, 1980; COOK and MULLINS, 1983; GAWTHORPE, 1986; YOSE and HELLER, 1989; DROMART *et al.*, 1993). Although the primary mechanisms responsible for such collapses and debris flows are still a topic of debate, correlative features of occurrences of megabreccia/conglomerates with sea-level fluctuations in other sections suggest that they may have been controlled by basin-wide events, e.g., sea-level falls or/and tectonic uplift.

Massive slides and slumps, which are other forms of allochthonous debris, are observed in the upper Sandaogou Formation of Qinglongshan and other stratigraphic intervals. Such sediments tend to be generated on low-angle mud-dominated slopes (HUNT and TUCKER, 1993) during sea-level fall (HILBRECHT, 1989; DROMART *et al.*, 1993). Highstand shedding, observed in modern sediments in the Bahamas (DROXLER and SCHLAGER, 1985; SCHLAGER *et al.*, 1994), may not be common in ancient rocks (VAIL *et al.*, 1991).

Thin-bedded lime mudstone of this association (Fig. 5-E) is distinguished from its basinal counterpart (Fig. 5-F) mainly by containing more terrigenous elements with a high proportion of silt-sized grain; it may have been deposited particularly on slopes and in basins close to land (STOW, 1994).

Basinal Lithofacies Association

The basinal lithofacies association consists of olive-green, dark-grey graptolitic shales, thin-bedded lime mudstones and distal fine-grained turbidites. This lithofacies association is well developed in the Pingliang Formation of Qinglongshan, the upper Qingshan Formation of Qingshan, and the middle Wangjiayuanzi Formation of Tianjingshan. In these horizons, the stratigraphic thicknesses are much thinner and turbidites are comparatively fewer, thinner and finer grained than those in the more proximal sections. Lime mudstone and shale form a relatively high proportion of the section. The thick megabreccias and other coarse, debris-flow deposits are usually rare to absent in this association.

Thin-bedded lime mudstone in this lithofacies association is characterized by well-developed planar bedding or laminar, and fine, thinner shelled fossils. Bioturbation is comparatively rare. Radiolaria usually are concentrated in some intervals of basinal

lime mudstones (Fig. 5-F). The thick shales are characterized by their olive-green to grey color, laminated character and well-preserved graptolites, which reflect condensed deposition (VAIL *et al.*, 1991), and were deposited below the zone of storm wave reworking, in a dyaerobic setting (GAWTHORPE, 1986). The clays may be transported by bottom-hugging nepheloid layers (BOARDMAN and NEUMANN, 1984) or dilute clouds.

Descriptions of the Sequences

Although synchroneity and generic controls of the development of sequences are still controversial (MIAL, 1992), sequence stratigraphy does provide a useful approach to construct the age-model, and to recognize the predictable lithofacies succession for examining depositional basins (SARG, 1988; VAIL, *et al.*, 1991; POSAMENTIER and JAMES, 1993; CHRISTIE-BLICK and DRISCOLL, 1995).

We recognized the sequences and systems tracts by: (1) regional subaerial or marine erosion surfaces, including stratigraphic hiatuses indicated by fossils; (2) abrupt shifts of lithofacies associations (e.g., drowning unconformity); and (3) the stacking styles of lithofacies associations between two unconformities. In addition, biostratigraphic data were also useful in distinguishing the coeval sequences and systems tracts between different sections, as no spatially continuous outcrops and seismic data could be utilized in our study.

By all these means, at least six sequences have been identified in the Ordovician of central Ningxia, together with two poorly-developed sequences at the bottom and top of the succession (Fig. 6-A, B, C). We summarize the characteristics of the sequences in the study area below.

Sequence 1

This sequence comprises the Xialingnangou Formation in the Qinglongshan section, with a thickness of about 36 m and in the Tianjingshan section, with a thickness of more than 60 m. The boundaries of the sequence are only distinguishable at Qinglongshan, where the lower sequence boundary is a flooding surface, indicated by an abrupt shift from overlying shallow subtidal-intertidal stromatolite boundstone to deeper, subtidal, thin-bedded dolostone. This sequence boundary may coincide with the Cambrian-Ordovician boundary (Fig. 2) according to the conodont data (LIU, 1991). The upper sequence boundary there, corresponding to an erosional surface, is represented by overlying solution collapse breccia, quartz sands, and a stratigraphic hiatus (see below for further discussion). At Tianjingshan, however, this sequence is a thrust block between the Tianjingshan Formation and the Wangjiayuanzi Formation (LIU, 1991), and thus no sequence boundaries have been recognized there.

The sequence at Qinglongshan includes two subsequences, both of which consist of lower, thin-bedded dolostone grading upward into cryptalgal laminites with shallowing-upward trend. The sequence at Tianjingshan consist chiefly of peloidal grainstone, though the relative sea-level curve of the Xialingnangou Formation there

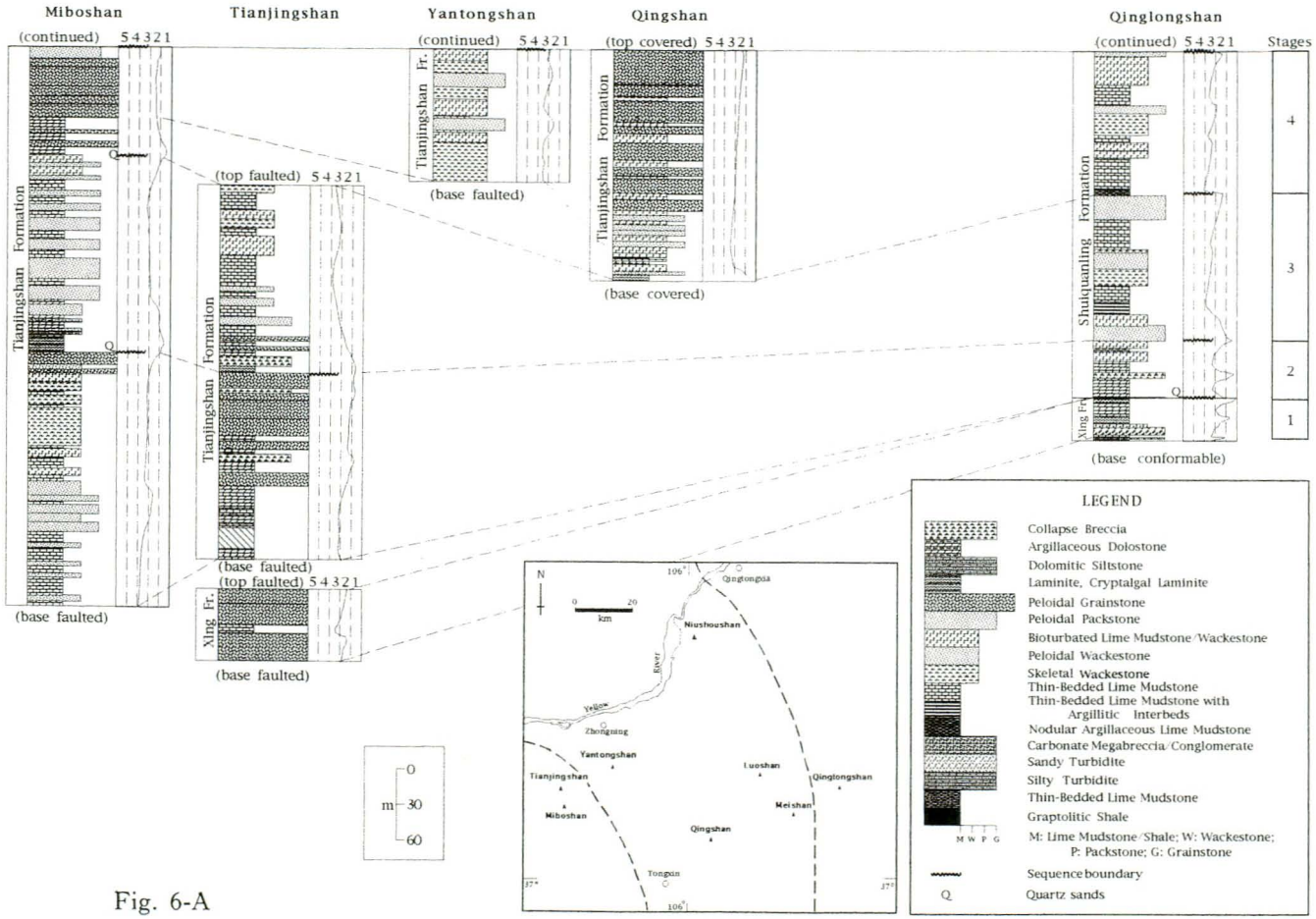
Miboshan
(continued) 5 4 3 2 1
Tianjingshan Formation
Q
(base faulted)
Tianjingshan
(top faulted) 5 4 3 2 1
Tianjingshan Formation
(base faulted)
(top faulted) 5 4 3 2 1
Xing Fr.
(base faulted)
Yantongshan
(continued) 5 4 3 2 1
Tianjingshan Fr.
(base faulted)
Qingshan
(top covered) 5 4 3 2 1
Tianjingshan Formation
(base covered)
Qinglongshan
(continued) 5 4 3 2 1
Shuiquanling Formation
Q
Xing Fr.
(base conformable)
Stages
4
3
2
1
m
0
30
60
N
0 20
km
Yellow River
Qinglongxia
Niushoushan
Zhongning
Yantongshan
Tianjingshan
Miboshan
Luoshan
Qinglongshan
Meishan
Qingshan
Tongxin
106°
37°
LEGEND
Collapse Breccia
Argillaceous Dolostone
Dolomitic Siltstone
Laminite, Cryptalgal Laminite
Peloidal Grainstone
Peloidal Packstone
Bioturbated Lime Mudstone/Wackestone
Peloidal Wackestone
Skeletal Wackestone
Thin-Bedded Lime Mudstone
Thin-Bedded Lime Mudstone with Argillitic Interbeds
Nodular Argillaceous Lime Mudstone
Carbonate Megabreccia/Conglomerate
Sandy Turbidite
Silty Turbidite
Thin-Bedded Lime Mudstone
Graptolitic Shale
M W P G
M: Lime Mudstone/Shale; W: Wackestone; P: Packstone; G: Grainstone
Sequence boundary
Q
Quartz sands

Fig. 6-A

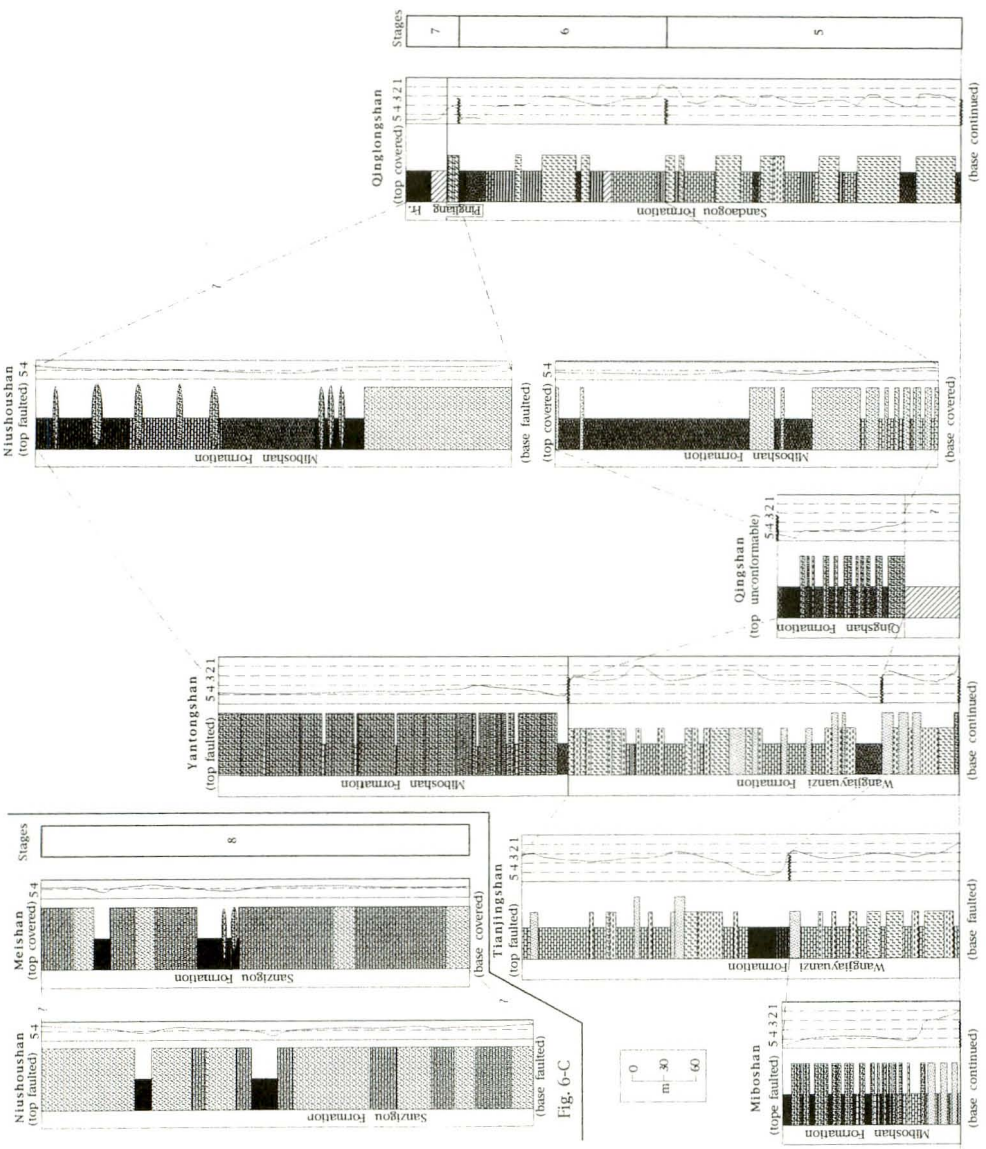

Fig. 6-B

Fig. 6. Sedimentary logs of the Ordovician in central Ningxia. Numbers above curves of relative sea-level fluctuations refer to various depositional settings: 1-peritidal, 2-shallow subtidal, 3-deeper subtidal, 4-basin-marginal, and 5-basinal environments. Inset map shows the location of the stratigraphic columns. Fig. 6-A: stratigraphic columns of the Tremadocian and the Arenigian, * Xln Fr. is abbreviated from Xialingnangou Formation; Fig. 6-B: stratigraphic columns of the Llanvirnian and the early Llandeilian; Fig. 6-C: stratigraphic columns after the Llandeilian.

suggests a depositional pattern similar to that at Qinglongshan (Fig. 6-A).

The subsequences of the sequence are fourth-order sequences with durations less than 1 Ma, which normally corresponds to parasequences. However, poor preservation of this sequence prevents further distinction into individual sequences at present.

Sequence 2

Sequence 2 includes the lower Shuiquanling Formation at Qinglongshan and the lower Tianjingshan Formation at Miboshan and Tianjingshan. Although the sequence varies in thickness from 31.8 m at Qinglongshan to about 214 m at Miboshan, the strata comprising this sequence can be correlated with other localities by the presence of the *Aurilobodus leptosomatus-Loxodus dissectus* conodont assemblage-zone, and with a probably similar duration of about 3.5 Ma. The basal sequence boundary at Qinglongshan is a erosional unconformity marked by solution collapse breccia with abundant quartz sands, whereas this boundary in the Zoulang Transitional Belt has been faulted (Fig. 6-A). The upper boundary of the sequence is distinguishable at all three sections as an exposure surface.

This sequence consists of two subsequences, as in sequence 1. The lower subsequence consists of thin-bedded dolostone capped by solution collapse breccia at Tianjingshan and Qinglongshan. At Miboshan, the lateral equivalent is composed of lower, deeper subtidal lime mudstone and bioturbated lime mudstone, overlain by shallow subtidal peloidal packstone/wackestone. The upper subsequence, however, comprises deeper subtidal bioturbated lime mudstone/wackestone, skeletal wackestone and thin-bedded lime mudstone with shallowing-upward trend at Qinglongshan and Miboshan. At Tianjingshan peloidal grainstone was deposited after the development of thinner peritidal sediments (Fig. 6-A).

The depocenter of the sedimentary basin during this episode may have been situated at Miboshan, which is suggested by variations of sequence thicknesses as well as of lithofacies styles.

Sequence 3

Sequence 3 comprises the middle Shuiquanling Formation of Qinglongshan and the middle Tianjingshan Formation at Tianjingshan and Miboshan. Its thickness varies from about 120 m up to 170 m, increasing from Qinglongshan to Miboshan. The sequence had a duration of about 3 Ma. The basal boundary of the sequence is an emergent surface, indicated by the well-developed vuggy voids at the top of the underlying bioturbated lime mudstone/wackestone at Qinglongshan, and by abundant quartz clastics in peritidal sediments above the basal sequence boundary at Miboshan. At Tianjingshan, the development of solution-collapse breccia at the base of the sequence may represent the coeval exposure event. The upper sequence boundary was recognized at Miboshan and Qinglongshan.

This sequence can be subdivided into three lithofacies subunits. At Tianjingshan

and Miboshan, the lowermost strata of the sequence are dominated by peritidal lithofacies association (cryptalgal laminites, dolomite and dolomitic siltstone) (Fig. 4-A). The middle subunit there is composed of lime mudstone and peloidal wackestone, and the upper unit there consists of bioturbated lime mudstone, peloidal wackestone and thin-bedded lime mudstone. At Qinglongshan, the lower subunit is represented by peloidal packstone grading upward into bioturbated lime mudstone. The middle and upper subunits consist of the subtidal lithofacies association (e.g., thin-bedded lime mudstone, peloidal wackestone, skeletal wackestone). However, the differentiation of the middle and upper unit there is quite difficult, if not impossible (Fig. 6-A).

The peritidal sediments (first subunit) on the Tianjingshan-Miboshan platform and, possibly, the coeval subtidal deposits with deepening-upward trend at Qinglongshan, are interpreted as the transgressive systems tract (TST) of the sequence. The highstand systems tract (HST) is much thicker and better developed than the transgressive systems tract within the study area. It is represented by deeper subtidal deposits in the most study sections, showing the shallowing-upward trend.

Sequence 4

This sequence is well represented in most of the carbonate platform sections within the study area, and probably had a duration of 3 Ma. It includes the upper Shuiquanling Formation at Qinglongshan, the upper Tianjingshan Formation at Miboshan, and the Tianjingshan Formation at Yantongshan and Qingshan. The thickness of the sequence varies from 91 m (at Miboshan) to 195 m (at Qingshan), suggesting that the depocenter of central Ningxia moved from Miboshan and Tianjingshan eastwards to Qingshan. The basal boundary of the sequence was recognized from the Miboshan and Qinglongshan sections. At Miboshan, that boundary, an exposure surface is marked by the overlying peritidal sediments with abundant quartz clastics, whereas at Qinglongshan it is marked by the deepening event, a drowning unconformity in the sense of SCHLAGER and CAMBER (1986).

Sequence 4 at Miboshan and Qingshan is represented by similar stacking patterns (Fig. 6-A) with the lower peritidal lithofacies association grading upward into shoal complexes. In contrast, the sequence exposed at Yantongshan and Qinglongshan consists mainly of deeper subtidal lithofacies associations with shallow subtidal peloidal packstone interbeds.

As in sequence 3, the lowermost peritidal sediments of the sequence at Miboshan and Qingshan are attributed to the transgressive systems tract of the sequence. The same systems tract at Qinglongshan may be represented by the lowermost argillaceous nodular lime mudstone and overlying thin-bedded lime mudstone, which may have been deposited during a period of rapid sea-level rise. The highstand systems tracts of the sequence are represented by shoal complexes at Miboshan and Qingshan, which can possibly be correlated with intensively bioturbated lime mudstone/wackestone at Yantongshan and Qinglongshan.

Sequence 5

This sequence comprises the lower Sandaogou Formation at Qinglongshan, the Miboshan Formation at Miboshan and the lower Wangjiayuanzi Formation at Tianjingshan and Yantongshan. Its thickness varies from less than 75 m at Yantongshan to more than 280 m at Qinglongshan, which indicates the further eastward movement of the depocenter of the sedimentary basin. The duration of this sequence may have been 4 Ma. The basal sequence boundary is manifested by an exposure surface which at Miboshan is associated with the interbeds of cryptalgal laminites andpeloidal packstone. At Yantongshan, the corresponding boundary is more dramatically indicated by a lag-conglomerate interval. At Qinglongshan, the lower boundary of the sequence can be recognized by a drowning event and synchronic invasion of cold-water fauna (AN and ZHENG, 1989). This boundary has been either covered or faulted at other sections in the study area. The deposition of the sequence was ended by an exposure event.

At Miboshan, the sequence consists of two lithofacies subunits (Fig. 6-B): lower, peritidal-shallow subtidal sediments and overlying basinal-marginal lithofacies association. The latter is composed of varied lithofacies but characterized by polygenic carbonate conglomerate/breccia induced by debris flows. At Yantongshan, the sequence can be differentiated into three subunits: the lowermost lag conglomerates with siltstone and less carbonate grainstone clastics, peritidal laminites and yellowish green siltstone; the overlying, deeper subtidal bioturbated lime mudstone/skeletal wackestone; and the upper, peloidal packstone intercalated with bioturbated lime mudstone. At Qinglongshan, the sequence is dominated by the deeper subtidal lithofacies association, and we cannot distinguish it into any subunits, except for the lowermost part which may be separated from the rest by the well-developed argillaceous nodular lime mudstone deposited during the period of the rapid sea-level rise. Finally, at Tianjingshan, although the basal part of the sequence has been faulted off, the lowermost dolostone suggests that the coeval sea-level fall event may also have controlled the deposition there.

The basin-marginal deposits of the Miboshan Formation at Miboshan are attributed to the lowstand systems tract of the sequence; at Yantongshan the coeval succession is represented only by about 5.0 m thick lag deposits. Sediments overlying the lag conglomerates at Yantongshan and the nodular, limestone enriched succession at Qinglongshan are interpreted as the transgressive systems tract of the sequence, representing a further rise of sea level. After the development of transgressive systems tract, sedimentation continued with a retrograding package of shallow, subtidal lithofacies association at Yantongshan, and deeper subtidal lithofacies association at Tianjingshan and Qinglongshan, which are attributed to a highstand systems tract of this sequence.

Sequence 6

Sequence 6 is composed of the upper Sandaogou Formation at Qinglongshan, the lower Miboshan Formation at Niushoushan, the Qingshan Formation at Qingshan and

the upper Wangjiayuanzi Formation at Tianjingshan and Yantongshan. This sequence varies in thickness from about 120 m at Qingshan to more than 360 m at Niushoushan. The basal bounding of this sequence is subtly marked by abrupt lithofacies changes, from thick-bedded peloidal packstones to black shale at Tianjingshan and to thin-bedded lime mudstone at Yantongshan. At Qinglongshan, however, the sea-level fall event is represented by overlying shallow subtidal sediments with abundant shallow-water bores as well as by the deposition of overlying peritidal laminates after the exposure event.

The succession of this sequence at Tianjingshan and Miboshan consists of two subunits (Fig. 6-B): the lowermost basinal lithofacies association (black shale and thin-bedded lime mudstone) and the overlying, deeper subtidal lithofacies association. The sequence at Qingshan and Niushoushan, though lithofacies are different, is composed of lower basin-marginal lithofacies and upper basinal lithofacies. At Qinglongshan, the well-developed laminites are interpreted as having been formed in relatively restricted environments, and the overlying, deeper, subtidal lithofacies association developed during the corresponding sea-level rise.

Spatially, the lowstand systems tract of the sequence consists of the basin-marginal lithofacies associations exposed at Qingshan and Niushoushan. The transgressive systems tract of the sequence is thin and poorly developed, and is represented by the basinal sediments at Tianjingshan and Yantongshan as well as by the peritidal laminites deposited at Qingshan. In contrast, the highstand systems tract is well developed and is represented by upper subunits (deeper subtidal lithofacies association) at Tianjingshan, Yantongshan and Qingshan. At Qingshan and Niushoushan, however, transgressive and highstand systems tracts of the sequence are hardly distinguished, where basinal shale and thin-bedded lime mudstone are interpreted as condensed TST/HST, which may have been common in deep-water environments (JAMES *et al.*, 1989; VAIL *et al.*, 1991).

Sequence 7

This sequence includes the uppermost Sandaogou Formation and the overlying Pingliang Formation at Qinglongshan, the upper Miboshan Formation at Niushoushan and the Miboshan Formation at Yantongshan. Its thickness varies from 57 m at Qinglongshan to more than 470 m at Yantongshan. The lower boundary of the sequence cannot be distinguished from most sections, but at Qinglongshan the basal boundary of the slump deposits is interpreted as the lower sequence boundary. This sequence at Yantongshan is dominated by more than 300 m thick carbonate conglomerates with polygenic clastics (Fig. 4-D). Rocks of the sequence at Qinglongshan, however, can be divided into two subunits (Fig. 6-B): 11 m-thick carbonate slump deposits and overlying basinal shales. At Niushoushan this sequence is represented by the lower, coarse, sandy turbidites and the upper basinal black shale and thin-bedded lime mudstone with carbonate conglomerate lenses.

The massive carbonate conglomerates of the Yantongshan section may be deposited

along the slope of a carbonate platform during sea-level fall, and are then labeled as a lowstand systems tract; similar systems tract is indicated by the coarse, sandy turbidites of Niushoushan and carbonate slump deposits of Qinglongshan. The transgressive systems tract and the highstand systems tract of the sequence were developed at Qinglongshan and Niushoushan as basinal sediments, but it is difficult to distinguish them from each other because of their condensed features.

Sequence 8

Sediments of this period, defined by the *Nemagraptus gracilis* graptolite biozone, have been known only from the Niushoushan, Meishan and Luoshan sections. No sequence boundary has been distinguished in the field. We here tentatively attribute these sediments as forming one sequence. Both successions are characterized by upward-fining sands or silts or mudstones/shales (Fig. 6-C). Bouma divisions were well developed there (Fig. 4 B). Compared with Luoshan and Meishan, the strata at Niushoushan generally contain thicker, coarser and more abundant beds of sandy turbidite.

Evolution of the Sequences and Paleogeography

As documented above, the Ordovician of central Ningxia have been subdivided into eight successive depositional sequences. We summarize the evolutionary patterns for each of these episodes below. The horizontal distributions of lithofacies and their associations at the end of each stage are illustrated in Figure 7 (Stage 1-Stage 8). However, as no palinspastic restoration has been attempted in this study, the actual basin should have been wider than that shown in this figure.

By the end of the Cambrian, early Caledonic Movement ended the slope-and-basinal depositions (Xiangshan Group) in the Zoulang Transitional Belt, and the marginal area of the Sino-Korean Platform (represented by the Qinglongshan section in the study area) kept the peritidal settings.

Stage 1 (early Tremadocian)

Early Tremadocian depositions have been known from only two separate localities in the study area, the other areas being interpreted as tectonic highlands. The paleogeography in this episode may still follow from the Late Cambrian but it differed from the Middle Cambrian in that a carbonate platform had developed in the Zoulang Transitional Belt at least from early Tremadocian. Deposition at the beginning of this stage was marked by a deepening event recorded in the lowest part of the Xialingnangou Formation of Qinglongshan, and then graded into peritidal deposition. At least two such shallowing-upward cycles with a duration of about 1 Ma of each, were distinguished from the succession of this stage at Qinglongshan. At the same time, shallow-water and wave-agitated sediments occurred in the Tianjingshan Formation, the southwestern study area, which may be related to the development of the adjacent highlands

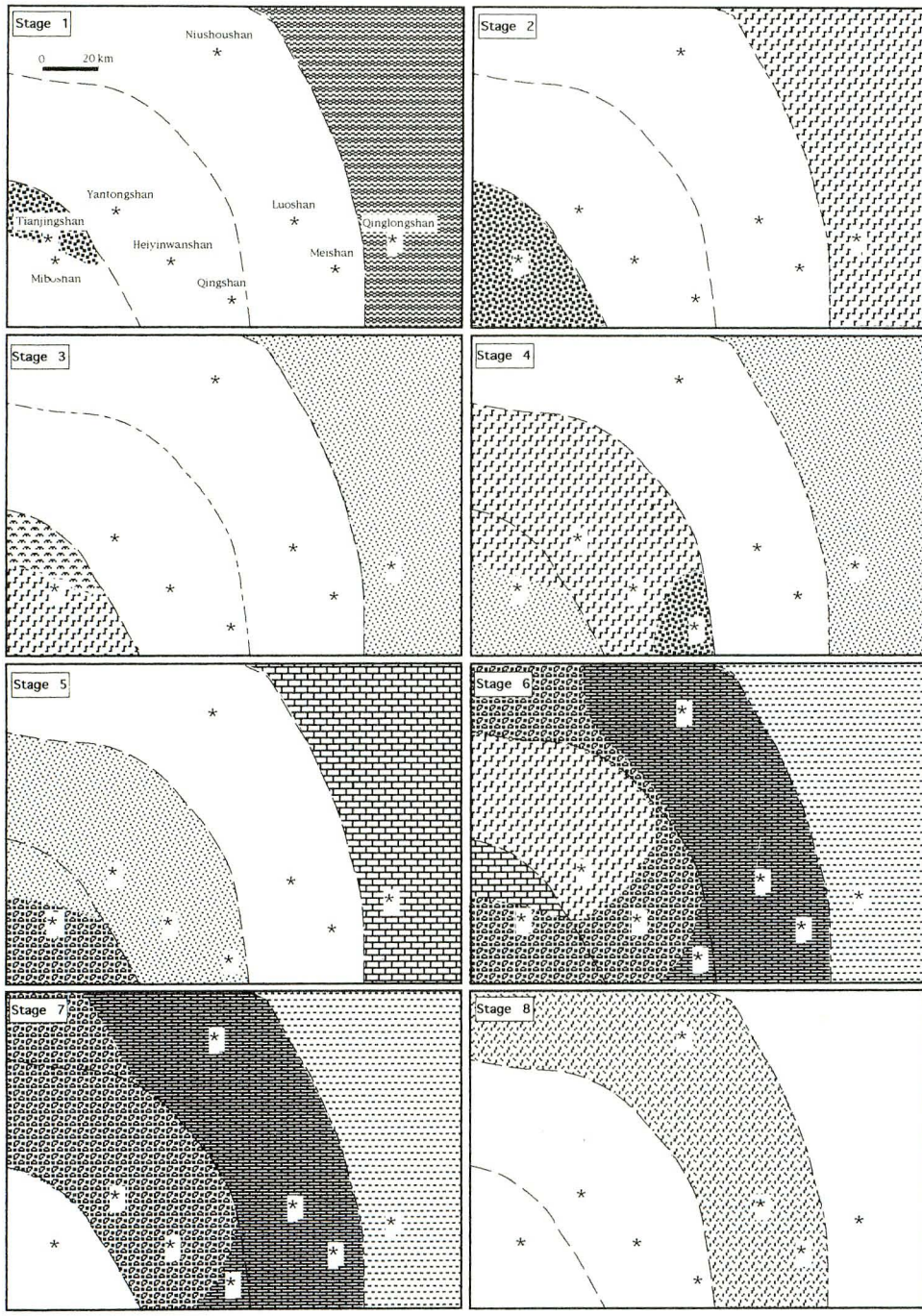

Fig. 7. Paleogeographic constructions showing distribution of depositional environments during successive stages of the Ordovician in central Ningxia. Lithofacies patterns are the same as those in Fig. 6, except dashed areas which refer to shaly basin and white areas which refer to highlands or later eroded areas.

(Fig. 7, Stage 1).

Stage 2 (middle Arenigian)

The development of the unconformity at the beginning of this episode represents a much more significant hiatal break (about 10 Ma) in the Ordovician succession, when much of the Tremadocian and lower Arenigian strata were removed in the study area (Fig. 2). A coeval unconformity has also been documented within the Ordovician succession on the Sino-Korean Platform, where the hiatus increases in magnitude from north to south (AN, 1986). The unconformity has usually been attributed to tectonic activation within the southern Qinling Fold Belt and the northern Inner Mongolian Fold Belt surrounding the Sino-Korean craton. We, however, argue that this stratigraphic lacuna may at least be partly attributed to the eustatic falling event, because the succeeding transgressive phase has already been well documented in the North American craton (BOVA and READ, 1987; KNIGHT and JAMES, 1987) and other cratons (NICOLL *et al.*, 1992), and interpreted as a global eustatic event (FORTEY, 1984; NIELSEN, 1992).

The paleogeographic framework of this stage shows a comparable pattern to that of stage 1. From middle Arenigian time, the eastern Qinglongshan and western Tianjingshan-Miboshan carbonate platforms were initially inundated again. One relative sea-level fall event has been recognized in the middle of the episode after retrograding sedimentation on the Tianjingshan-Miboshan and Qinglongshan carbonate platforms. The sedimentary environment became deeper and more extensive later, and shoal settings then dominated the flooding areas in response to the decelerated rise of accommodation space. Other areas may have still remained emergent throughout this stage (Fig. 7, Stage 2). The depocenter of the sedimentary basin during this stage was situated in the western study area (Miboshan locality) as represented by thicker and well-developed subtidal sediments lacking peritidal characteristics.

Stage 3 (from middle to late Arenigian)

The paleogeographic geometry at this stage succeeded from its former stage. The sea-level fall event at the beginning of this stage induced the exposure surface bounding the base of the sequence, and then peritidal deposition reoccurred at the Tianjingshan-Miboshan carbonate platform, corresponding to the flooding of the central Ningxia area. At Tianjingshan, quartz clastics in peritidal sediments above the sequence boundary mark intense erosion in the surrounding emerged highlands. The eastern area, on the other hand, is dominated by a shallow-water depositional setting, which can be ascribed to the higher subsidence rate there. At a later stage, shoal sediments prograded onto the flooding area, reflecting the later phase of the sea-level rise (Fig. 7, Stage 3). The deposition of this stage was ended by a sea-level fall event, which triggered the formation of the upper boundary of this sequence.

Stage 4 (late Arenigian)

The paleogeographic geometry of this stage succeeded from stage 3, but the western carbonate platform extended to Yantongshan as well as to Qingshan. The depocenter of the basin likely moved eastwards from Miboshan, which may be an indication of tectonic activity within the North-Qilian Fold Belt. This sequence represents the development of the largest carbonate platforms in central Ningxia during the Ordovician.

The beginning of this stage is marked by an abrupt deepening, drowning unconformity at Qinglongshan. Such drowning unconformities have been documented from various stratigraphic horizons and tectonic provenances, but the controlling factor attributed to this kind of stratigraphic surface is still a subject of debate (READ *et al.*, 1991; SCHLAGER, 1992; RANKEY *et al.*, 1994). As the deposition of carbonate was not hindered at other sections (Fig. 6-A), the short-term, rapid, sea-level rise may have controlled the development of the drowning type of the lower sequence boundary at Qinglongshan instead of the environmental crisis of carbonate production.

After deposition of the poorly-developed transgressive systems tracts, a regressive stratigraphic pattern, represented by shoal sediments, was deposited in the study area, corresponding to a decelerated sea-level rise (Fig. 7, Stage 4).

Stage 5 (from the end of Arenigian to early Llanvirnian)

The onset of this sequence is characterized by the occurrence of slope deposits at Miboshan (Fig. 7, Stage 5), while other areas remained as developments of the carbonate platform. Such profound paleogeographic inversion was initiated by the re-active tectonics in this area, which is also verified by the deposition of bentonites at this stage. However, the peritidal settings at Miboshan occurred again before the deposition of the basin-marginal lithofacies associations. In addition, the lower sequence boundary of the sequence at Qinglongshan coincides with the turnover from warm-water conodont fauna to cold-water conodont fauna (AN and ZHENG, 1989) and with an abrupt sedimentary shift from shoal deposits to nodular argillaceous mudstone. All these evidence also suggests that tectonic activity only is not enough to interpret the origin of the boundary of this sequence, though it may indeed induce the formation of Miboshan slope. Thus we argue that the eustatic rise, combined with a little late tectonic activity could have induced the abrupt changes of sedimentary settings and the turnover of the conodont fauna.

At this stage the depocenter of the basin may have moved further east to Qinglongshan, with a rapid subsidence rate in response of the thrusting load of the collision of the North-Qilian Fold Belt with North China. In the western study area, long-term upward-shoaling successions were developed (Fig. 6-B) until interrupted by a carbonate drowning event.

Stage 6 (late Llanvirnian)

From the beginning of this stage, the basin-marginal deposition on slopes surrounding the carbonate platform or ramp extended from Miboshan to Qingshan and Niushoushan,

which suggests further tectonic activity (Fig. 7, Stage 6). The basin-marginal clastics in the Miboshan Formation of Niushoushan may have been derived from north-west Alxa Oldland (LIANG, 1992), whereas the carbonate clastics, eroded from various stratigraphic intervals, were probably transported from adjacent carbonate platforms by debris flows. The abrupt basinward shift of lithofacies associations at the beginning of this stage at Tianjingshan and Yantongshan reflects the demise of the carbonate platform as a result of rapid sea-level rise after exposure or sea-level fall (RANKEY *et al.*, 1994). The coeval sea-level fall event is also indicated by the surface between the subtidal sediments with abundant shallow-water bores and the overlying laminites at Qinglongshan.

In response to the deceleration of sea-level rise, shallow-water carbonates began to dominate the Tianjingshan-Yantongshan platform again, while at Qinglongshan the relative sea level became deeper in the long term. We attribute such a deepening-upward sedimentary trend as an result of an increasing subsidence rate. In the deep-water setting of Qingshan and Niushoushan then, only fine-grained sediments were deposited, in contrast to the deposition of coarse debris flows and turbidites during lower sea level (Fig. 7, Stage 6).

Stage 7 (Early Llandeilo)

At the beginning of this stage, a new phase of tectonic activity ended the development of the Tianjingshan-Yantongshan carbonate platform and hindered the carbonate deposition at Qinglongshan (Fig. 6-B). The basal boundary of this sequence may also be attributed to a sea-level fall event, which is probably contemporary sea-level fall event, recognized from the southeastern margin of the Ordos Basin as well as from the North America craton shelf margin as documented by ROSS and ROSS (1992).

The carbonate megabreccia/conglomerates (more than 400 m thick) indicate the development of depositional slopes and associated sediment instability on the seafloor during this time. The abundant terrigenous clastics at Niushoushan were induced by medium- to low-concentration turbidite flows, whereas the overlying thin-bedded lime mudstone and black shales mark the condensed deposits during the higher sea-level interval. At Qinglongshan, the lowermost carbonate slump sediments were deposited during lower sea-level stand. The overlying graptolitic shales are responses of increasing influx of fine-grained terrigenous material in this area (Fig. 7, Stage 7).

Stage 8 (from late Llandeilo to early Carodocian)

The paleogeography of this stage is reconstructed as a deep, elongate trough with a south-north trend, extending at least from Niushoushan to Luoshan (including Meishan). The other areas of central Ningxia may have been exposed (Fig. 7, Stage 8).

Strata younger than this stage have not discovered in the central Ningxia area.

Conclusions

This study has resulted in the documentation of sequences and paleogeographic

evolution of the Ordovician basin in central Ningxia. In synthesis, we propose the following evolutionary history of the basin:

The early deposits of the Ordovician may have continued from the end of the Cambrian in peritidal to shallow subtidal environments. After extensive erosion and exposure, the Qinglongshan and Tianjingshan-Miboshan carbonate platforms were inundated again due probably to global eustatic rise from the middle Arenigian. In the following Arenigian, sedimentation of central Ningxia was dominated by cyclic, shallow-water carbonates, but was interrupted by long-term sea-level fall events. From the beginning of the Llanvirnian, tectonic re-activity led to abrupt changes in the paleogeographic framework and may also have generated sequence boundaries, together with eustatic fluctuations. Basin-marginal deposits were first deposited at Miboshan, then at Qingshan and Yantongshan, and at Tianjingshan-Niushoushan, in turn, indicating that the Tianjingshan-Miboshan carbonate platform was destroyed gradually from southwest to northeast. The contemporary deposition at Qinglongshan, on the other hand, became deeper due both to the thrusting load of North-Qilian Fold Belt and to the eustatic rise. From the beginning of the Middle Ordovician, carbonate sedimentation in central Ningxia was hindered, possibly by the increasing influx of terrigenous materials at a lower sea level.

The enhanced tectonic activity of the North-Qilian Fold Belt may have uplifted all this area above sea-level from early Caradocian, after the last development of the Niushoushan-Luoshan Trough.

Acknowledgments

Acknowledgement is made to the donors of the Grants for Doctor Course to the Department of Geology, Peking University, administered by the National Education Committee of P.R. China, for the partial support of this research. The manuscript was significantly improved by the critical reviews of Professor YAO Akira and Associate Professor MAEJIMA Wataru of Osaka City University.

References

AIGNER, D.K., 1985, Storm depositional systems: dynamic stratigraphy in modern and ancient shallow-marine sequences. *Lecture Notes in Earth Science*, v. 3, Berlin, Springer-Verlag, 174p.

AN, T., 1986, Recent process in Ordovician System of North China. In: *Selected Paper from Department of Geology*. Peking University (1984), Geological Publishing House, p. 44–58. (in Chinese with English abstract)

AN, T. and ZHENG, Z., 1989, The Conodonts of the Marginal Areas Around the Ordos Basin, North China. Science Press, 201 p. (in Chinese with English abstract)

BERGSTRÖM, S.M., 1977, Early Paleozoic biostratigraphy in the Atlantic Borderland. In: SWAIN, G.M., ed., *Stratigraphic Micropaleontology of Atlantic Basin and Borderlands*. Elsevier Science Publishing Company, Amsterdam, p. 85–110.

BOVA, J.A. and READ, J.F., 1987, Incipiently drowned facies within a cyclic peritidal ramp sequence, Early Ordovician Chepultepec interval, Virginia Appalachians. *Geological Society of America Bulletin*, v. 98, p. 714–727.

BURCHETTE, T.P., WRIGHT, V.P. and FAULKNER, T.J., 1990, Oolitic sandbody depositional models and

geometries, Mississippian of southwest Britain: implications for petroleum exploration in carbonate ramp settings. *Sedimentary Geology*, v. 68, p. 87–115.

COOK, H.E. and MULLINS, H.F., 1983, Basin margin environments. In: Scholle, P.A., Bebout, D.E., and Moore, C.H., eds., *Carbonate Depositional Environments*. American Association of Petroleum Geologists Memoir 33, p. 539–617.

CREVELLO P.D. and SCHLAGER, W., 1980, Carbonate debris sheets and turbidites, Exuma Sound, Bahamas. *Journal of Sedimentary Petrology*, v. 50, p. 1121–1148.

CUI, G., ZHANG, C. and WANG, S., 1985, Evolutionary features of Helanshan aulacogen. In: *The Records of Geological Research*. Peking University Press, p. 39–47. (in Chinese with English abstract)

de RAAF, J.F.M., BOERSMA, J.R. and van GELDER, A., 1977, Wave-generated structures and sequences from a shallow marine succession, Lower Carboniferous, County Cork, Ireland. *Sedimentology*, v. 24, p. 451–483.

DROMART, G., FERRY, S. and ATROPS, F., 1993, Allochthonous deep-water carbonates and relative sea-level changes: the Upper Jurassic-Lowermost Cretaceous of southeast France. In: POSAMENTIER, H.W., SUMMERHAYES, C.P., HAQ, B.U. and ALLEN, G.P., eds., *Sequence Stratigraphy and Facies Associations*. Spec. Publs Int. Ass. Sediment. 18, p. 295–305.

DROXLER, A.W. and SCHLAGER, W., 1985, Glacial versus interglacial sedimentation rates and turbidite frequency in the Bahamas. *Geology*, v. 13, p. 799–802.

ENOS, P. and PERKINS, R.D., 1977, *Quaternary Sedimentation in South Florida*. Geological Society of America Memoir 147, 198p.

FORTEY, R.A., 1984, Global earlier Ordovician transgressions and regressions and their biological implications. In: BRUTON, D.L., ed., *Aspects of the Ordovician System*. Palaeontological Contributions from the University of Oslo no. 295, Universitesforlaget, p. 37–50.

FORTEY, R.A., HARPER, D.A.T., INGHAM, J.K., OWEN, A.W. and RUSHTON, A.W.A., 1995, A revision of Ordovician series and stages from the historical type area. *Geological Magazine*, v. 132, p. 15–30.

GAWTHORPE, R.L., 1986, Sedimentation during carbonate ramp-to-slope evolution in a tectonically active area: Bowland Basin (Dinantian), North England. *Sedimentology*, v. 33, 185–206.

GE, M., ZHENG, Z. and LI, Y., 1991, Research on Ordovician and Silurian Graptolites and Graptolite-Bearing Strata from Ningxia and the Neighbouring Districts. Nanjing University Press, 199p. (in Chinese)

GOLDHAMMER, R.K., LEHMANN, P.J. and DUNN, P.A., 1993, The origin of high-frequency platform carbonate cycles and third-order sequences (Lower Ordovician El Paso GP, west Texas): constraints from outcrop data and stratigraphic modeling. *Journal of Sedimentary Petrology*, v. 63, p. 318–359.

HARDIES L.A. and SHINN, E.A., 1986, Carbonate depositional environments, modern and ancient: Part 3: Tidal flats. *Colorado School of Mines Quarterly*, v. 81, p. 1–74.

HARLAND, W.B., ARMSTRONG, R.L., COX, A.V., CRAIG, L.E., SMITH, A.G. and SMITH, D.G., 1989, *A Geologic Time Scale*. New York, Cambridge University Press, 128p.

HILBRECHT, H., 1989, Redeposition of Late Cretaceous pelagic sediments controlled by sea level fluctuations. *Geology*, v. 17, p. 1072–1075.

HINE, A.C., WILBUR, R.J. and NEUMANN, A.C., 1981, Carbonate sand bodies along contrasting shallow bank margins facing open seaways in northern Bahamas. *American Association of Petroleum Geologists Bulletin*, v. 65, p. 262–290.

HUNT, D. and TUCKER, M.E., 1993, Sequence stratigraphy of carbonate shelves with an example from the mid-Cretaceous (Urgonian) of southeast France. In: POSAMENTIER, H.W., SUMMERHAYES, C.P., HAQ, B.U., and ALLEN, G.P., eds., *Sequence Stratigraphy and Facies Associations*. Spec. Publs Int. Ass. Sediment. 18, p. 307–341.

HUO, S. *et al.*, 1989, Introduction to Geology of Ningxia. Science Press, 155p. (in Chinese)

JAMES, N.P., 1984, Shallowing-upward sequences in carbonates. In: WALKER, R.G., ed., *Facies Models* (2nd edition). Geoscience Canada Reprint Series 1, p. 213–228.

JAMES, N.P., STEVENS, R.K., BARNES, C.R. and KNIGHT, I., 1989, Evolution of a Lower Paleozoic continental margin carbonate platform, Northern Canadian Appalachians. In: CREVELLO, P.D., WILSON, J.L., SARG, J.F., and READ, J.F., eds., *Controls on Carbonate Platform and Basin Developments*. Society Economic Paleontologists Mineralogists Special Publication 44, p. 123–146.

KENDALL, C.G.St.C. and SCHLAGER, W., 1981, Carbonates and relative changes in sea-level. *Marine Geology*, v. 44, p. 181–212.

KNIGHT, I. and JAMES, N.P., 1987, The stratigraphy of the Lower Ordovician St. George Group, western Newfoundland: the interaction between eustasy and tectonics. *Canadian Journal of Earth Sciences*, v. 24, p. 1927–1951.

LIANG, C., 1992, Stratigraphic and Sedimentary Study of Paleozoic (Cambrian-Ordovician) in Middle Southern

Margin of North China Platform (unpublished report), 129p. (in Chinese)

LINDSTRÖM, M., 1971, Lower Ordovician succession of conodont fauna. Report International Geological Congress, 21st, v. 7, p. 88–96.

LIU, J., 1991, Sedimentary facies and conodont biofacies of the Ordovician in middle west margin of Ordos Basin, North China (unpublished M.Sc. thesis). Department of Geology, Peking University, Beijing, 193p. (in Chinese with English abstract)

MIALL, A.D., 1992, Exxon global cycle chart: an event for every occasion?. *Geology*, v. 20, p. 787–790.

MULLINS H.J., NEUMANN, A.C., WILBER, R.J., HINE, A.C. and CHINBURG, S.J., 1980, Carbonate sediment drifts in the northern straits of Florida. *American Association of Petroleum Geologists Bulletin*, v. 64, p. 1701–1717.

NICOLL, R.S., NIELSEN, A.T., LAURIE, J.R. and SHERGOLD, J.H., 1992, Preliminary correlation of latest Cambrian to Early Ordovician sea level events in Australia and Scandinavia. In: WEBBY, B.D., and LAURIE, J.R., eds., *Global Perspectives on Ordovician Geology*. Balkema, Rotterdam, p. 381–394.

NIELSEN, A.T., 1992, Intercontinental correlation of the Arenigian (Early Ordovician) based on sequence and ecostratigraphy. In: WEBBY, B.D., and LAURIE, J.R., eds., *Global Perspectives on Ordovician Geology*. Balkema, Rotterdam, p. 367–379.

OSLEGER, D.A. and READ, J.F., 1991, Relation of eustasy to stacking patterns of meter-scale carbonate cycles, Late Cambrian, U.S.A.. *Journal of Sedimentary Petrology*, v. 61, p. 1225–1252.

OSLEGER, D.A. and READ, J.F., 1993, Comparative analysis of methods used to define eustatic variations in outcrop: Late Cambrian interbasinal sequence developments. *American Journal of Science*, v. 293, p. 157–216.

POSAMENTIER, H.W. and JAMES, D.P., 1993, An overview of sequence-stratigraphic concepts: uses and abuses. In: POSAMENTIER, H.W., SUMMERHAYES, C.P., HAQ, B.U., and ALLEN, G.P., eds., *Sequence Stratigraphy and Facies Associations*. Spec. Publs Int. Ass. Sediment. 18, p. 3–18.

PRATT, B.R. and JAMES, N.P., 1988, The St. George Group (Lower Ordovician) of western Newfoundland: tidal flat island model for carbonate sedimentation in shallow epeiric seas. *Sedimentology*, v. 33, p. 313–343.

PURDY, E.G., 1963, Recent calcium carbonate facies of the Great Bahama Bank. 2. Sedimentary facies. *Journal of Geology*, v.71, p. 472–497.

RANKEY, E.C., WALKER, K.R. and SRINIVASAN, K., 1994, Gradual establishment of Iapentan "passive" margin sedimentation: stratigraphic consequences of Cambrian episodic tectonism and eustasy, Southern Appalachians. *Journal of Sedimentary Research*, v. B64, p. 298–310.

READ, R.J., OSLEGER, D.A. and ELRICK, M.A., 1991, Two-dimensional modeling of carbonate ramp sequences and component cycles. In: FRANSEEN, E.K., WATNEY, W.L., KENDALL, C.G.St.C., and ROSS, W., eds., *Sedimentary Modeling: Computer Simulations and Methods for Improved Parameter Definition. Kansas Geological Survey Bulletin*, v. 97, p. 1054–1069.

READING, H.G., 1978, *Sedimentary Environments and Facies*. New York, Elsevier, 557p.

ROSS J.P. and ROSS, C.A., 1992, Ordovician sea-level fluctuations. In: WEBBY, B.D., and LAURIE, J.R., eds., *Global Perspectives on Ordovician Geology*. Balkema, Rotterdam, p. 327–335.

SARG, J.F., 1988, Carbonate sequence stratigraphy. In: WIGUS, C.K., HASTINGS, B.S., KENDALL, C.G.St.C., POSAMENTIER, H.W., and Van WAGONER, J.C., eds., *Sea Level Changes: An Integrated Approach*. SEPM Special Publication 43, p.155–181.

SCHLAGER, W., 1992, *Sedimentology and sequence stratigraphy of reefs and carbonate platforms*. American Association of Petroleum Geologists, Continuing Education Course Notes 34, 71p.

SCHLAGER, W. and CAMBER, O., 1986, Submarine slope angles, drowning unconformities, and self-erosion of limestone escarpments. *Geology*, v. 14, p. 762–765.

SCHLAGER, W., RIJMER, J.J.G. and DROXLER, A., 1994, Highstand shedding of carbonate platforms. *Journal of Sedimentary Research*, v. B64, p. 270–281.

STOW, D.A.V., 1994, Deep sea processes of sediment transport and deposition. In: PYE, K., ed., *Sediment Transport and Depostional Processes*. Blackwell Scientific Publications, Oxford, p. 257–291.

TUCKER, M.E., CALVET, F. and HUNT, D., 1993, Sequence stratigraphy of carbonate ramps: systems tracts, models and application to the Muschelkalk carbonate platforms of eastern Spain. In: POSAMENTIER, H.W., SUMMERHAYES, C.P., HAQ, B.U., and ALLEN, G.P., eds., *Sequence Stratigraphy and Facies Associations*. Spec. Publs Int. Ass. Sediment. 18, p. 397–415.

VAIL, P.R., AUDEMARD, F., BOWMAN, S.A., EISNER, P.N. and PEREZ-CRUZ, C., 1991, The stratigraphic signatures of tectonics, eustasy and sedimentology-an overview. In: EINSELE, G., RICKEN, W., and SEILACHER, A., eds., *Cycles and Events in Stratigraphy*, p. 617–659.

WANLASS, H.R., 1979, Limestone response to stress: pressure solution and dolomitization. *Journal of*

Sedimentary Petrology, v. 49, p. 437–462.

WILLIAMS, A., STRACHAN, I., BASSETT, D.A., DEAN, W.T., INGHAM, J.K., WRIGHT, A.D. and WHITTINGTON, H.B., 1972, *A Correlation of the Ordovician Rocks in the British Isles*. Geological Society of London Special Report no. 3, 74p.

YOSE, L.A. and HELLER, P.L., 1989, Sea-level control of mixed-carbonate-siliciclastic, gravity-fllow deposition: Lower part of the Keeler Canyon Formation (Pennsylvanian), southeastern California. *Geological Society of America Bulletin*, v. 101, p. 427–439.